Chemical Science

ROYAL SOCIETY OF CHEMISTRY

EDGE ARTICLE

View Article Online
View Journal | View Issue

Cite this: *Chem. Sci.*, 2024, **15**, 17481

All publication charges for this article have been paid for by the Royal Society of Chemistry

Received 7th May 2024
Accepted 17th September 2024

DOI: 10.1039/d4sc02982h

rsc.li/chemical-science

Direct observation of β-alkynyl eliminations from unstrained propargylic alkoxide Cu(I) complexes by C–C bond cleavage†

Ba L. Tran, * Jack T. Fuller, III, Jeremy D. Erickson, Bojana Ginovska* and Simone Raugei *

β-Carbon eliminations of aryl, allylic, and propargylic alkoxides of Rh(I), Pd(II), and Cu(I) are key elementary reactions in the proposed mechanisms of homogeneously catalysed cross-coupling, group transfer, and annulation. Besides the handful of studies with isolable Rh(I)-alkoxides, β-carbon eliminations of Pd(II)- and Cu(I)-alkoxides are less definitive. Herein, we provide a comprehensive synthetic, structural, and mechanistic study on the β-alkynyl eliminations of isolable secondary and tertiary propargylic alkoxide Cu(I) complexes, LCuOC(H)(Ph)C≡CPh and LCuOC(Ar^F)$_2$C≡CPh (L = N-heterocyclic carbene (NHC), dppf, *S*-BINAP), to produce monomeric (NHC)CuC≡CPh, dimeric [(diphosphine)CuC≡CPh]$_2$, and the corresponding carbonyl. Selective β-alkynyl over β-hydrogen elimination was observed for NHC- and diphosphine-supported secondary propargylic alkoxide complexes. The mechanism for the first-order reaction of β-carbon elimination of (IPr*Me)CuOC(Ar^F)$_2$C≡CPh is proposed to occur through an organized four-centred transition state *via* a Cu-alkyne π complex based on Eyring analysis of variable-temperature reaction rates by UV-vis kinetic analysis to provide $\Delta H^{\ddagger}$ = 24(1) kcal mol^{-1}, $\Delta S^{\ddagger}$ = −8(3) e.u., and $\Delta G^{\ddagger}$ (25 °C) = 27 kcal mol^{-1} over a temperature range of 60–100 °C. Additional quantitative UV-vis kinetic studies conclude that the electronic and steric properties of the NHC ligands engendered a marginal effect on the elimination rate, requiring 2–3 h at 100 °C for completion, whereas complete β-alkynyl eliminations of diphosphine-supported propargylic alkoxides were observed in 1–2 h at 25 °C.

Introduction

The elucidation of mechanisms and selectivities for reactions catalysed by Earth abundant first-row metals is critical to the development of sustainable organotransition chemistry.[1–5] The elementary reactions of β-carbon elimination from metal-alkyl and -alkoxide intermediates are prominent in olefin polymerization and catalytic C–C bond formations.[6–9] Specifically, the β-eliminations of allyl,[9] alkynyl,[10–20] and aryl groups[17,21–23] from unstrained alkoxides of Pd and Rh to generate the corresponding organo-Pd and -Rh intermediates are implicated in the mechanism of cross-coupling, annulation, and aryl shuttling catalysis.[8,9] To date, only a handful of synthetic and mechanistic studies of β-carbon elimination from alkoxide Rh complexes have been reported.[21–24] Besides Pd and Rh, Cu-mediated β-allyl[25] and β-alkynyl eliminations[26–28] of allylic alcohols and propargylic alcohols to generate allyl and acetylide intermediates in catalytic allyl group transfer and annulation reactions have been proposed, yet definitive spectroscopic, structural or mechanistic evidence remains unreported to our knowledge.

In contrast to the vast literature on the related mechanism of β-hydrogen elimination, experimental examples and mechanistic knowledge of β-carbon elimination are less established.[6–9] The formation of π complexes with allyl, alkynyl, or aryl ligands can be favorable compared to that of M–H–C σ-complexes. However, the reorganization of the larger carbon groups at a metal centre compared to the small spherical H atom of the C–H group is kinetically disfavored. Because of the mechanistic similarities of these two elimination pathways, selective promotion of β-carbon elimination over β-hydrogen elimination is not fully understood, yet is of synthetic interest.[8]

We direct our studies towards the β-alkynyl eliminations of propargylic alcohols at Cu(I) centres because of the broad interest in Cu-acetylide chemistry in catalysis and inorganic materials.[29–32] Moreover, the stability of Cu-acetylide is ideal for product isolation in combination with spectroscopic, structural, and mechanistic investigation.[33–35] Based on experimental and computational mechanistic analysis of β-carbon eliminations of

Institute for Integrated Catalysis, Pacific Northwest National Laboratory, Richland, WA 99352, USA. E-mail: ba.tran@pnnl.gov; bojana.ginovska@pnnl.gov; simone.raugei@pnnl.gov

† Electronic supplementary information (ESI) available: Synthetic details, spectroscopic characterisation, and details of kinetics studies (PDF). CCDC 2345818 **1-Me**, 2345810 **1-OMe**, 2345819 **1-Cl**, 2345809 **2-Me**, 2345811 **2-OMe**, 2345814 **2-Cl**, 2345817 **4**, 2345816 **5**, 2345813 **8a**, 2345812 **8b**, 2345815 **9**. For ESI and crystallographic data in CIF or other electronic format see DOI: https://doi.org/10.1039/d4sc02982h

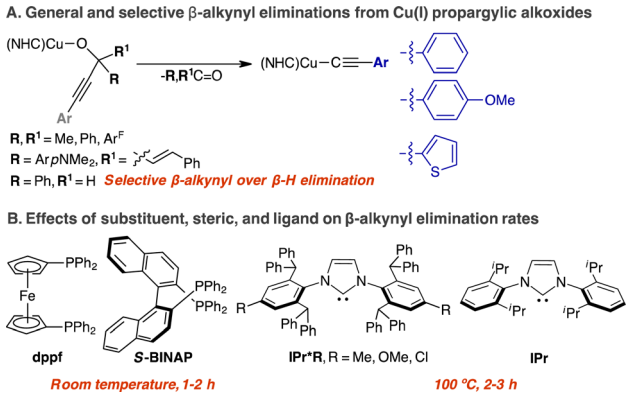

Scheme 1 This work details a comprehensive study on the general and selective β-alkynyl eliminations of secondary and tertiary propargylic alkoxides of Cu(I).

unstrained alkoxide Rh complexes,[17,22,23,36] we envision a coordinatively unsaturated Cu(I) centre can coordinate and activate the alkyne group at the propargylic alkoxide *via* a Cu(I)-alkyne π complex to promote β-alkynyl elimination. Herein, we report a rare comprehensive study detailing the synthesis, structure–reactivity relationship, and mechanism of β-alkynyl eliminations from two- and three-coordinate propargylic alkoxide Cu complexes supported by electronically and sterically varied NHCs and diphosphines (Scheme 1).

Results and discussion

Synthesis, characterisation, and β-alkynyl elimination of (NHC)Cu(I) propargylic alkoxides

A series of tertiary propargylic alkoxide complexes, (IPr*R)CuOC(Ar^F)$_2$C≡CPh (R = Me, **1-Me**; OMe, **1-OMe**; Cl, **1-Cl**), were isolated in 73–80% by treating the corresponding (IPr*R)CuCl with 1.05 equiv. of NaN(SiMe$_3$)$_2$ in toluene for 0.5 h, followed by addition of solid HOC(Ar^F)$_2$C≡CPh for another 1 h at 25 °C (Scheme 2). Subsequent removal of NaCl by filtration and layering of pentane over the toluene reaction mixture at 25 °C over 24–48 h gave analytically clean, off-white crystalline products of **1-Me**, **1-OMe**, and **1-Cl**. Synthetic procedures with accompanying ^{1}H, ^{13}C{^{1}H}, and ^{19}F{^{1}H} NMR data are provided in the ESI (pg. S3–S8†). The propargylic alkoxide complexes

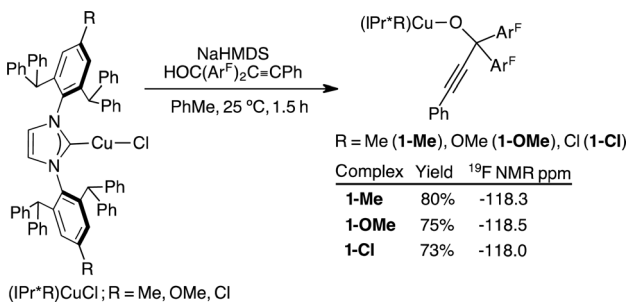

Complex	Yield	^{19}F NMR ppm
1-Me	80%	-118.3
1-OMe	75%	-118.5
1-Cl	73%	-118.0

Scheme 2 Synthesis and ^{19}F{^{1}H} NMR spectroscopic data of (IPr*R)CuOC(Ar^F)$_2$C≡CPh.

exhibit similar spectroscopic and structural properties; we therefore discuss the characterisation of (IPr*Me)CuOC(Ar^F)$_2$-C≡CPh (**1-Me**) as a representative example.

The ^{19}F{^{1}H} NMR spectrum of **1-Me** contains a sharp singlet at −118 ppm, shifting upfield upon complexation from free HOC(Ar^F)$_2$C≡CPh at −115 ppm. The −118 ppm signal is diagnostic for the formation of CuOC(Ar^F)$_2$C≡CPh and is insensitive to the identity of IPr*R ligands (Scheme 2). The ^{1}H NMR spectrum shows a multiplet at 8.03 ppm corresponding to the C–H group *ortho* to the C–O group of the propargyl alkoxide. The alkynyl and C–O functionalities are identified by ^{13}C NMR resonances at 101, 83 and 77 ppm, respectively.

The single crystal X-ray diffraction (scXRD) structure of **1-Me**, shown in Fig. 2, verified its linear geometry. Standard bond distances of 1.8586(16) Å and 1.8094(13) Å were observed for Cu1–C1 and Cu1–O1, respectively. The C1–Cu1–O1 angle of 163.46(7)° of **1-Me** is notably bent compared to those of related IPr*Me-supported alkoxides and allylic alkoxides at 172–178°.[37,38] The distances from Cu1 to C3 and C4 of the alkyne group of 3.11 and 3.64 Å, respectively, do not support a Cu-alkyne π-complex, which exhibits a range of 1.95–1.99 Å for Cu(I)-alkyne.[39] The scXRD structure of **1-Cl** also contains a bent C1–Cu1–O1 angle at 162.77(5)° whereas the C1–Cu1–O1 angle for **1-OMe** is at 172.46(7)° (Fig. 2).

(IPr*Me)CuOC(Ar^F)$_2$C≡CPh (**1-Me**) is stable in C$_6$D$_6$ at room temperature during the monitoring time of 24 h by ^{1}H, ^{19}F{^{1}H} NMR spectroscopy. Subsequent thermolysis at 100 °C for 3 h quantitatively produced (IPr*Me)Cu(C≡CPh) (**2-Me**) and Ar$^F_2$C=O by ^{1}H, ^{19}F{^{1}H} NMR spectroscopy in the presence of a 1,3,5-trimethoxybenzene internal standard. ^{19}F{^{1}H} NMR spectroscopic analysis over time shows the consumption of **1-Me** at −118 ppm with concomitant growth of Ar$^F_2$C=O at −107 ppm, supporting the extrusion of Ar$^F_2$C=O from **1-Me** (Fig. S5B†). The product of **2-Me** was identified by the two doublets at 7.69 ppm (J = 7.5 Hz), 7.51 ppm (J = 7.7 Hz) and a triplet at 7.25 ppm (J = 7.7 Hz) by ^{1}H NMR spectroscopy (Fig. 1), consistent with reported ^{1}H NMR data for **2-Me** (ref. 33) and independently synthesized **2-Me** (Fig. S24A†). The elimination of Ar$^F_2$C=O from **1-Me** proceeds sluggishly at lower temperature. Thermolysis of **1-Me** at 50 °C for 1 h and 24 h produced 5% and 27% of **2-Me**, respectively.

The β-alkynyl elimination is irreversible as the insertion reaction of Ar$^F_2$C=O and **2-Me** to regenerate **1-Me** was not observed after 48 h at 25 °C by ^{1}H and ^{19}F{^{1}H} NMR spectroscopy.[40] The scXRD structural determination of **1-Me** (Fig. 2), from the preparative-scale thermolysis of **1-Me** in toluene at 100 °C for 3 h, provided unequivocal evidence of the β-alkynyl elimination reaction. Analogously, the thermolysis of **1-OMe** and **1-Cl** in C$_6$D$_6$ at 100 °C for 3 h also cleanly produced (IPr*OMe)CuC≡CPh (**2-OMe**) and (IPr*Cl)CuC≡CPh (**2-Cl**), respectively, and Ar$^F_2$C=O (Fig. S6 and S7†). The spectroscopic assignments of **2-OMe** and **2-Cl** were verified by independent synthesis along with spectroscopic (Fig. S25 and S26†) and structural characterisation (Fig. 2).

We next evaluated whether reducing the steric congestion at the Cu(I) centre of the propargylic alkoxide complex by employing a less bulky NHC, such as IPr, relative to IPr*Me can

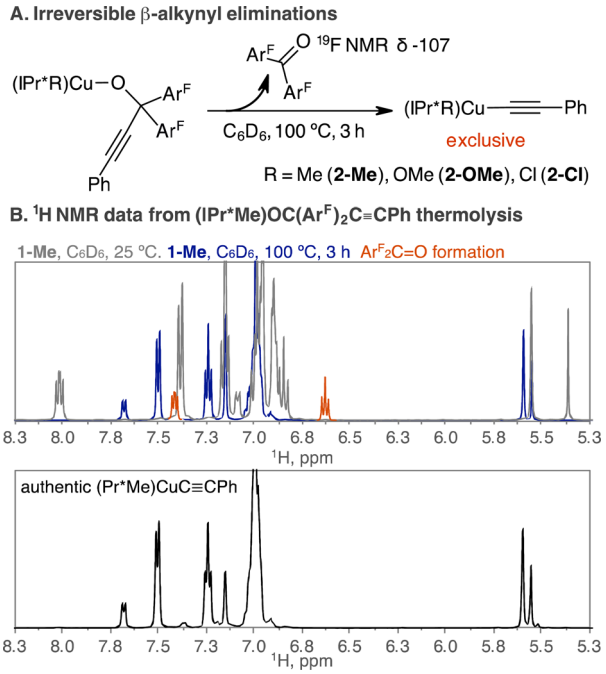

Fig. 1 (A) Thermolysis of (IPr*R)CuOC(Ar^F)$_2$C≡CPh produced the products (IPr*R)CuC≡CPh and Ar^F$_2$C=O. (B) The formation of Ar^F$_2$C=O and (IPr*Me)CuC≡CPh (**2-Me**) was identified (top) and verified using independently synthesized **2-Me** by ^{1}H NMR spectroscopy (bottom).

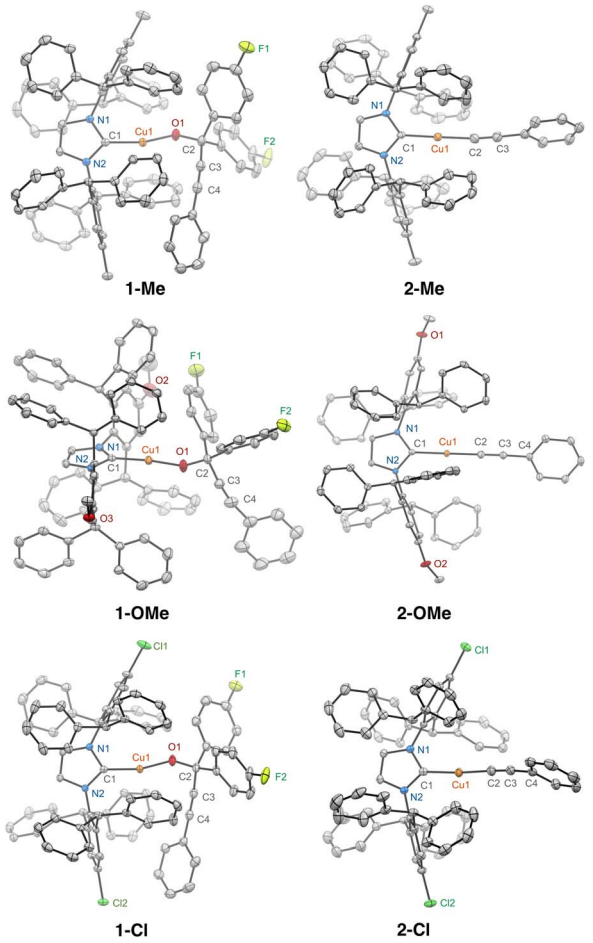

Fig. 2 scXRD structures of (IPr*R)CuOC(Ar^F)$_2$C≡CPh (**1-Me**, **1-OMe**, **1-Cl**) and (IPr*R)CuC≡CPh (**2-Me**, **2-OMe**, **2-Cl**) are shown at a 50% probability thermal ellipsoid. All hydrogen atoms, positional disorders, and solvents are omitted. Metrical parameters of these complexes are mostly similar; therefore, we list selected bonds (Å) and angles (°) of **1-Me** and **2-Me**: **1-Me**, Cu1–C1 = 1.8586(16) and Cu1–O1 = 1.8094(13); C3–C4 = 1.200(3); C1–Cu1–O1 = 163.46(7) and Cu1–O1–C2 = 128.06(12). **2-Me**, Cu1–C1 = 1.8869(13), Cu1–C2 = 1.8809(16), and C2–C3 = 1.190(2); C1–Cu1–C2 = 172.07(6) and Cu1–C2–C3 = 171.20(15).

facilitate the formation of a Cu(I)-alkyne π complex to lower the energy barrier for β-alkynyl elimination based on the isolation of a Rh(I)-arene π complex from the β-aryl elimination of a Rh(I)-alkoxide.[23] To do so, we isolated (IPr)CuOC(Ar^F)$_2$C≡CPh (**3**) in 65% and examined its reactivity (Fig. S4 and S8†). Similar to the (IPr*R)CuOC(Ar^F)$_2$C≡CPh series, **3** is stable in C_6D_6 at 25 °C over 24 h, and complete conversion of **3** to (IPr)CuC≡CPh and Ar^F$_2$C=O required heating at 100 °C for 3 h based on ^{1}H and ^{19}F {^{1}H} NMR spectroscopic analysis. A quantitative UV-vis kinetic analysis of the steric properties of NHC ligands is reported in a later section.

Diphosphines enabled β-alkynyl eliminations of LCuOC(Ar^F)$_2$C≡CPh (L = dppf, *S*-BINAP) at room temperature

Hartwig and co-workers structurally characterized the complex of (Et$_3$P)$_2$RhOC(Ph)$_2$(η^2-Ph), in which one of the phenyls of the triphenylmethoxide ligand contains a Rh-arene interaction, as a key intermediate en route to β-aryl elimination.[23] The same authors observed rapid β-alkynyl elimination of *in situ* generated trigonal planar (Et$_3$P)$_2$RhOC(Ph)$_2$C≡CPh at −40 °C,[17] in which it is plausible that β-alkynyl elimination proceeds by a Rh-alkyne π complex.

From these precedents and the observed stability of linear (IPr*R)CuOC(Ar^F)$_2$C≡CPh for β-alkynyl elimination, we postulate that diverting from NHC-supported linear propargylic alkoxides to diphosphine-supported trigonal planar propargylic alkoxide complexes might lower the energy barrier for β-alkynyl elimination by facilitating the formation of the Cu-alkyne π complex. This hypothesis aligns with the qualitative molecular orbital analysis and experimental studies that indicate geometric perturbation of a linear d^{10} configuration to a bent or trigonal configuration leads to higher reactivity.[41–44] Additionally, computation predicts that the pyramidalization of trigonal planar Cu(I) species to accommodate a coordinating ligand (*e.g.* alkyne group) occurs at lower energy than the bending of linear Cu(I) species.[45]

Indeed, treating (dppf)Cu(mesityl)[46] with 1.0 equiv. of HOC(Ar^F)$_2$C≡CPh in C_6D_6 at 25 °C produced [(μ-dppf)CuC≡CPh]$_2$ (**4**), Ar^F$_2$C=O, and a new species by the initial collection of the NMR spectroscopic data. As expected, the ^{31}P {^{1}H} NMR spectrum contains product **4** at −11 ppm, which has been spectroscopically characterized.[34] The ^{31}P{^{1}H} NMR signal at −21.8 ppm and the ferrocenyl ^{1}H NMR signals at 4.06 and

3.81 ppm in the $^{31}P\{^1H\}$ and ^1H NMR spectra (Fig. S9A and C†), respectively, indicate the formation of a new species. These signals do not correspond to free dppf, which contains a $^{31}P\{^1H\}$ NMR signal at −17.5 ppm and ^1H NMR signals of the ferrocenyl moiety at 4.14 and 4.03 ppm in C_6D_6. The $^{19}F\{^1H\}$ NMR spectrum shows a 1 : 3 ratio of $Ar^F{}_2C{=}O$ (−107 ppm) and the new species (−117 ppm) (Fig. S9B†), consistent with a $CuOC(Ar^F)_2C{\equiv}CPh$ species based on the $^{19}F\{^1H\}$ NMR data of (NHC)$CuOC(Ar^F)_2C{\equiv}CPh$ complexes (*see above*). From the collective multinuclear NMR data, we therefore proposed the formation of (dppf)$CuOC(Ar^F)_2C{\equiv}CPh$ as the new species.[47] After 1 h at 25 °C, only major products of **4** and $Ar^F{}_2C{=}O$ were detected by ^1H, $^{19}F\{^1H\}$, and $^{31}P\{^1H\}$ NMR spectroscopy (Fig. S9†). A preparative-scale reaction of *in situ* generated (dppf)Cu(mesityl) and $HOC(Ar^F)_2C{\equiv}CPh$ in toluene at 25 °C for 2 h produced **4** in an isolated yield of 60% by recrystallization from THF and pentane at 25 °C over 48 h. The ^1H and $^{31}P\{^1H\}$ NMR data of isolated **4** match those of **4** generated in the above elimination reaction and the reported literature (Fig. S10†).[34] Moreover, the scXRD structure of **4**, presented in Scheme 3, verifies its dimeric structure.

To demonstrate the generality of diphosphines for mediating β-alkynyl elimination at room temperature, we examined the reaction of *S*-BINAP, CuMes, and $HOC(Ar^F)_2C{\equiv}CPh$ in C_6D_6. After 2 h at 25 °C, the formation $[(S\text{-BINAP})CuC{\equiv}CPh]_2$ (**5**) and $Ar^F{}_2C{=}O$ was evidenced by ^1H, $^{19}F\{^1H\}$, $^{31}P\{^1H\}$ NMR spectroscopy (Fig. S11 and S12†). Vapor diffusion of pentane into the reaction mixture at 25 °C afforded yellow crystals of **5** in 52% isolated yields and scXRD structural determination for the dimer of **5** is shown in Scheme 3. Besides the effect of ligands on the rates of β-alkynyl elimination, X-ray crystallographic analysis also revealed the dependence of ligands on the nuclearity of the acetylide complexes in the solid state. Specifically, the preferred formations of monomeric and dimeric phenylacetylide complexes are supported by NHCs[33] and diphosphines,[35] respectively.

Scope and selectivity of β-alkynyl eliminations

Thus far, we have shown that NHC and diphosphine ligands can promote β-alkynyl eliminations of $LCuOC(Ar^F)_2C{\equiv}CPh$ complexes at different rates and temperatures. We next determined the scope for substituted propargylic alkoxides and the selectivity of β-alkynyl *versus* β-hydrogen elimination. The scope of propargylic alkoxide Cu(I) complexes for β-alkynyl elimination is summarized in Scheme 4.

The steric properties of the dimethyl and diphenyl groups at the β-carbon of the propargylic alkoxide were tolerated as evidenced by the clean conversion of (IPr*Me)$CuOC(Me)_2C{\equiv}CPh$ (**6a**) and (IPr*Me)$CuOC(Ph)_2C{\equiv}CPh$ (**6b**) to **2-Me** in C_6D_6 at 100 °C for 3 h (Scheme 4, Fig. S15 and S18†). Replacing phenylacetylene with electron-rich 4-methoxyphenyl acetylene or 2-thiophene acetylene in complexes of (IPr*Me)$CuOC(Ar^F)_2C{\equiv}C(C_6H_4\text{-}p\text{-}OMe)$ (**7a**) and (IPr*Me)$CuOC(Ar^F)_2C{\equiv}C(C_4H_3S)$ (**8a**) also underwent complete elimination to the corresponding acetylide products (IPr*Me)$CuC{\equiv}C(C_6H_4\text{-}p\text{-}OMe)$ (**7b**) and (IPr*Me)$CuC{\equiv}C(C_4H_3S)$ (**8b**) (Fig. S19, S20, S27, and S28†). The solid-state structures of **8a** and **8b** have been verified by scXRD measurement and are shown in Fig. 3. Detailed synthetic, spectroscopic, and structural characterisation of propargylic alkoxide complexes and acetylide products is provided in the ESI.†

The proposed stepwise reaction sequence of β-alkynyl elimination and 1,4-conjugate addition has enabled (BINAP)Rh-catalysed 1,3-alkynyl rearrangement of alkenyl carbinols to the

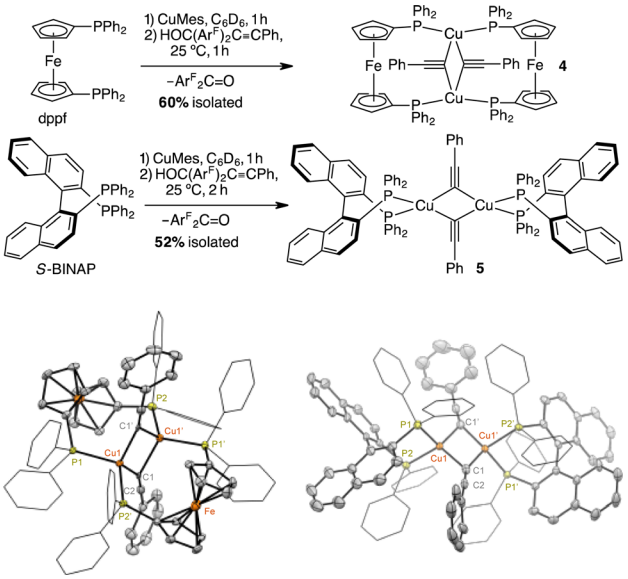

Scheme 3 scXRD structures of dimeric $[(\mu\text{-dppf})Cu(C{\equiv}CPh)]_2$ (**4**) and $[(S\text{-BINAP})Cu(C{\equiv}CPh)]_2$ (**5**) shown at a 50% probability thermal ellipsoid. All hydrogen atoms, positional disorders, and solvents are omitted.

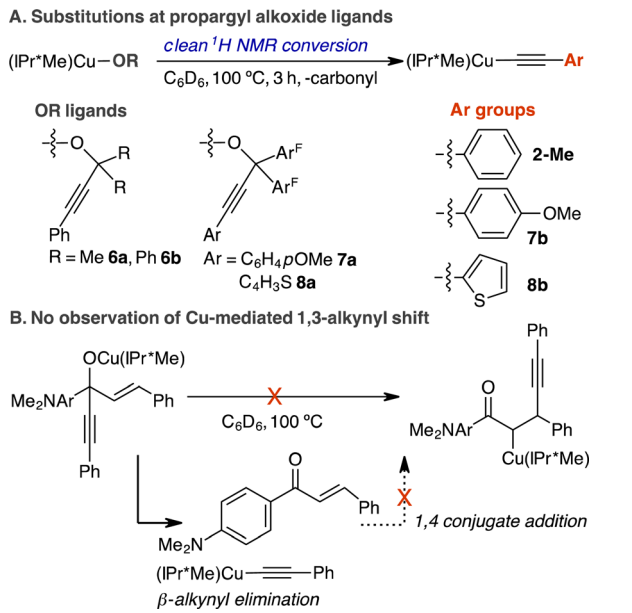

Scheme 4 (A) The scope of propargyl alkoxide complexes for β-alkynyl eliminations. (B) Probing for 1,3-alkynyl rearrangement in the reaction of (IPr*Me)$CuN(SiMe_3)_2$ and $HOC(C{\equiv}CPh)(C_6H_4\text{-}p\text{-}NMe_2)(-CH{=}CHPh)$ in C_6D_6, 100 °C, 3 h.

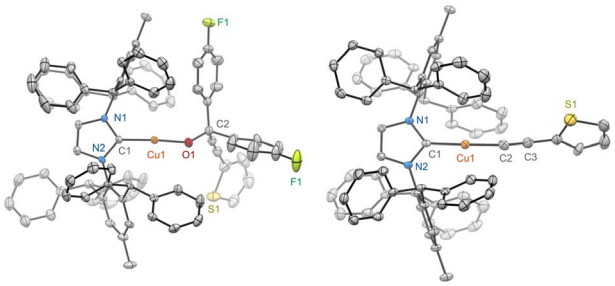

Fig. 3 scXRD structures of **8a** (left) and **8b** (right) are shown at a 50% probability thermal ellipsoid. All hydrogen atoms, positional disorders, and solvents are omitted.

corresponding β-alkynylketones.[14] Therefore, we investigated whether Cu(I) can mediate this 1,3-alkynyl rearrangement by examining the stoichiometric reaction of (IPr*Me)CuN(SiMe$_3$)$_2$, (dppf)CuMes or (*S*-BINAP)CuMes with 1.0 equiv. HOC(C≡CPh)(C$_6$H$_4$-*p*-NMe$_2$)(–CH=CHPh) in C$_6$D$_6$ at 25–100 °C for 3–24 h (Scheme 4B). ^{1}H, ^{31}P{^{1}H} NMR spectroscopic analysis of the reaction indicates only the formation of corresponding phenylacetylide complexes of **2-Me**, **4**, and **5**. Control reactions of isolated **2-Me**, **4**, or **5** with 1.0–2.0 equiv. of 3-(fluorophenyl)-1-phenyl-2-propen-1-one in C$_6$D$_6$ at 25–80 °C for 24–48 h produced no reactions. Collectively, these results indicate that the resulting NHC- or diphosphine-supported phenylacetylide Cu(I) complexes after β-alkynyl eliminations from propargylic alkoxides cannot engage the extruded α,β-unsaturated ketone in 1,4-conjugate addition to complete the 1,3-alkynyl rearrangement as previously observed for Rh chemistry.

To determine the selectivity of β-alkynyl and β-hydrogen elimination, we analyzed the thermolysis of secondary propargylic alkoxide complexes of LCuOC(H)(Ph)C≡CPh (L = IPr*Me, dppf). We hypothesized that β-alkynyl elimination can be selective over β-hydrogen elimination because the irreversible formation of Cu-acetylides from tertiary propargylic alkoxides hints at a highly exothermic reaction compared to the endothermic reaction of β-hydrogen elimination of Cu(I)-alkoxide to generate Cu–H as suggested by computation studies.[48] If β-alkynyl and β-hydrogen elimination traverses a similar four-centred transition state *via* a Cu-alkyne π or a Cu–H–C σ-complex, respectively, then the π-complex is likely favored over the σ-complex based on the varied reports of Cu-alkyne π complexes[29,39] and the computationally predicted repulsive nature of the Cu–H–C interaction.[49]

Analogous to **1-Me**, the secondary propargylic alkoxide complex of (IPr*Me)CuOC(H)(Ph)C≡CPh (**9**) is stable at 25 °C in C$_6$D$_6$ for 24 h by ^{1}H NMR spectroscopy.[50] Heating the C$_6$D$_6$ solution of **9** at 100 °C for 2 h and 4 h produced (IPr*Me)CuC≡CPh (**2-Me**) in 75% and 85%, respectively, against a 1,3,5-trimethoxybenzene internal standard, indicating selective β-alkynyl elimination (Fig. 4). The expected product of PhCHO was detected at 9.63 ppm and verified by spiking the post-reaction mixture with fresh PhCHO, leading to the growth of the 9.63 ppm signal. The presence of [(IPr*Me)CuH]$_2$ or metallic copper from [(IPr*Me)CuH]$_2$ decomposition or Cu-vinyl species

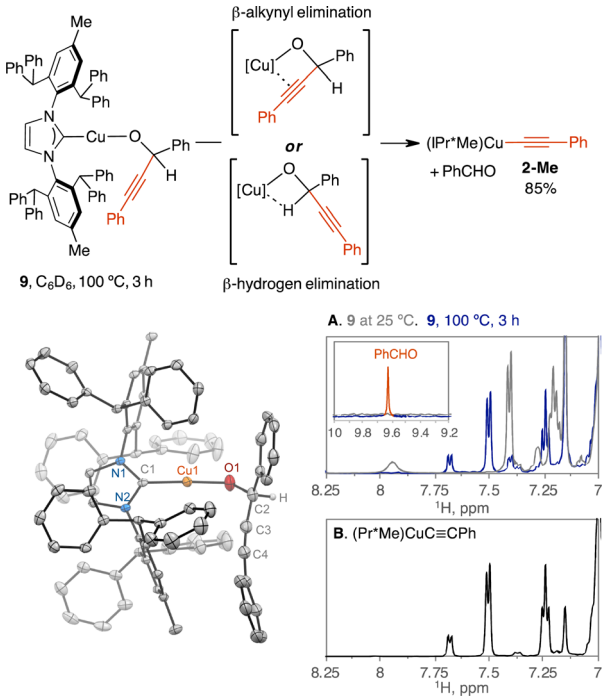

Fig. 4 Selective β-alkynyl over β-hydrogen elimination of compound **9** to products **2-Me** and PhCHO. (A) ^{1}H NMR data of **9** at 25 °C before heating and at 100 °C after 3 h, showing the presence of **2-Me** and PhCHO. (B) Verification of **2-Me** in the reaction by referencing the ^{1}H NMR spectrum of authentic **2-Me**. The scXRD structure of **9** is shown at a 50% probability thermal ellipsoid and the hydrogen atom on the alkoxide ligand was located and refined without constraint.

from alkyne insertion into the Cu–H bond was not spectroscopically observed (Fig. S22†).

Selective β-alkynyl elimination was also achieved in the reaction of dppf, CuMes, and HOC(H)(Ph)C≡CPh. The initial ^{1}H NMR spectrum (C$_6$D$_6$, 25 °C) after treating *in situ* generated (dppf)CuMes with HOC(H)(Ph)C≡CPh contained 58% of PhCHO and [(dppf)Cu(C≡CPh)]$_2$ (**5**), and a proposed new species of (dppf)CuOC(H)(Ph)C≡CPh based on resonances at 6.36 ppm and 4.13, 3.82 ppm corresponding to the C–H group of OC(H)(Ph)CCPh and ferrocenyl C–H of dppf (Fig. S23A†). After 1 h, the major products of PhCHO and **5** were observed in 95% by ^{1}H and ^{31}P{^{1}H} NMR spectroscopy (Fig. S23A and B†). These results demonstrate that the conserved selectivity of β-alkynyl over β-hydrogen elimination in secondary propargyl alkoxide Cu(I) complexes is independent of NHC and diphosphine ligands. Selective β-alkynyl elimination from a secondary propargylic alkoxide of (dppm)$_2$ReOC(H)(Ph)C≡CPh has been reported (dppm = bis(diphenylphosphino)methane).[51] However, the product of (dppm)$_2$ReC≡CPh was not isolated, as the acetylide complex underwent an acid-mediated secondary reaction to form a vinylidene complex.

Eyring analysis and the effect of NHC ligands on the rates of β-alkynyl elimination by quantitative UV-vis kinetic studies

Based on experimental and computational studies of β-aryl eliminations from Rh alkoxides,[22–24,36] β-alkynyl elimination of

(NHC)CuOC(Ar^F)$_2$C≡CPh likely proceeds through a four-centred transition state *via* a Cu-alkyne π complex, in which an associative mechanism for rate-limiting C–C bond cleavage should engender a negative entropy of activation $\Delta S^{\ddagger}$. Alternatively, a dissociative mechanism for the rate-limiting extrusion of Ar^F$_2$C=O from (NHC)CuC≡CPh(Ar^F$_2$C=O) after C–C bond cleavage should yield a positive $\Delta S^{\ddagger}$.

To distinguish these scenarios, we performed an Eyring analysis in a temperature range of 60–100 °C for the thermolysis of (IPr*Me)CuOC(Ar^F)$_2$C≡CPh (**1-Me**) in toluene to produce (IPr*Me)CuOC≡CPh (**2-Me**) and Ar^F$_2$C=O. The rates of β-alkynyl elimination, k_{obs}, were determined by UV-vis kinetic studies, in which the reaction progress was monitored at 355 nm for the formation of Ar^F$_2$C=O over 5–6 half-lives (Fig. 5). A representative UV-vis kinetic profile and plot of absorbance *versus* time for the first-order reaction of β-alkynyl elimination of 3.8 mM **1-Me** at 100 °C is shown in Fig. 5. Eyring analysis of the variable-temperature rate data provided activation parameters of $\Delta H^{\ddagger} = 24(1)$ kcal mol^{-1}, $\Delta S^{\ddagger} = -8(3)$ e.u., and $\Delta G^{\ddagger}$ (25 °C) = 27 kcal mol^{-1} (Fig. 5). A free energy of $\Delta G^{\ddagger}$ (25 °C) = 27 kcal mol^{-1} is consistent with the lack of β-alkynyl elimination of **1-Me** at room temperature. The magnitude and negative $\Delta S^{\ddagger}$ support an associative mechanism for the β-alkynyl elimination of **1-Me** and are consistent with reported Eyring analysis for unimolecular β-hydrogen and β-alkyl elimination of metal alkyl complexes that proceed through four-centred transition states.[52–55] We further demonstrated the unimolecular β-alkynyl elimination of **1-Me** in the solid state. Heating of solid **1-Me** at 100 °C under a N_2 atmosphere, followed by dissolution of the solid aliquots at the designated time intervals in C_6D_6 for ^{1}H, ^{19}F{^{1}H} NMR spectroscopic analysis, showed a mixture of **1-Me** and **2-Me** in ratios of 1.0 : 2.5, 1.0 : 8.0, and 1.0 : 25 after 3 h, 6 h and 9 h, respectively (Fig. S30†).

To determine the effect of steric and electronic properties of NHC ligands on β-alkynyl elimination of tertiary propargylic alkoxides, we measured the rates of elimination for 3.8 mM of **1-Me**, **1-Me**, **1-OMe**, **1-Cl** and **3** in toluene at 90 °C using the above UV-vis kinetic procedure. The resulting rates of reaction are summarized in Fig. 6. Complexes **1-Me** and **3**, which contain calculated %volume buried (r = 5.5 Å) of 63.6 for IPr*Me and 46.3 for IPr,[56] exhibited similar elimination rates of 2.6(1) × 10^{-4} s^{-1} and 2.4(1) × 10^{-4} s^{-1}, respectively, whereas electronically varied **1-OMe** and **1-Cl** underwent β-alkynyl elimination 2.2 and 1.3 times faster than that of **1-Me**, respectively. Additional studies to elucidate the electronic effects of **1-OMe** and **1-Cl** on the elimination rate were not pursued since the contribution is minor compared to diphosphines, which can promote β-alkynyl elimination at room temperature. Collectively, propargylic alkoxide complexes supported by diphosphines exhibited faster rates of β-alkynyl elimination at lower reaction temperature than those supported by sterically and electronically modified monodentate NHC ligands.

The accelerated β-alkynyl eliminations of diphosphine-supported propargylic alkoxide Cu(I) complexes at room temperature compared to those of NHC-supported propargylic alkoxide Cu(I) complexes at higher temperature is rationalized by a lowered energy barrier for C–C bond cleavage of the propargylic alkoxide from a three-coordinate propargylic alkoxide complex or a four-coordinate (diphosphine)Cu-alkyne

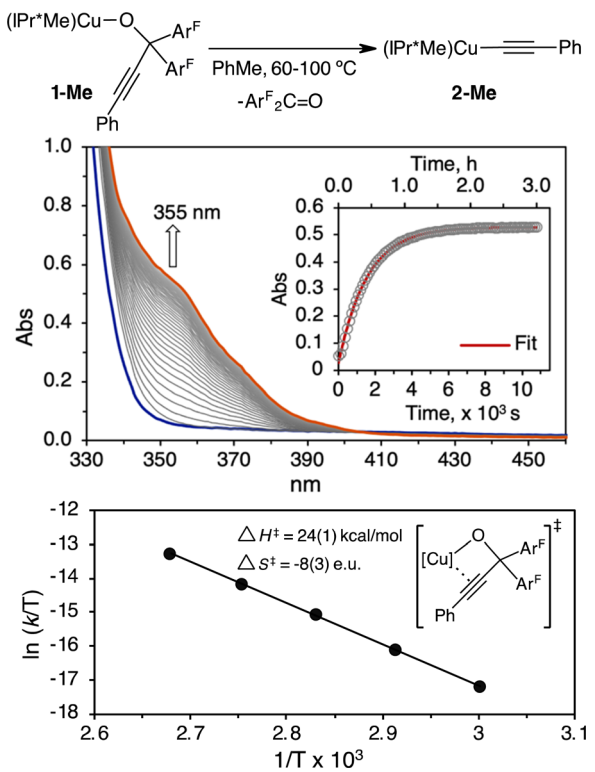

Fig. 5 UV-vis kinetic and Eyring analysis for the β-alkynyl elimination of **1-Me** (3.8 mM) support an associative mechanism. Representative UV-vis kinetic profile and analysis of **1-Me** (3.8 mM) in toluene at 100 °C indicate first-order kinetic behavior and a k_{obs} = 6.2 × 10^{-4} s^{-1}. A summary of all k_{obs} at 60–100 °C in duplicate runs is provided in Table S1 of the ESI.†

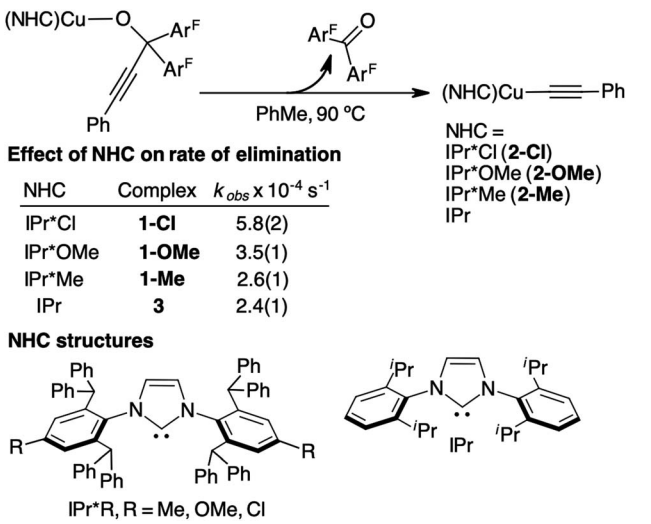

Fig. 6 A summary of UV-vis kinetic studies for the β-alkynyl elimination rates of 3.8 mM **1-Me**, **1-OMe**, **1-Cl**, and **3**. Additional UV-vis kinetic plots and duplicate or triplicate measurements of rates are provided in Fig. S29A–D and Table S2 of the ESI.†

π complex as the ground-state (GS) structure. To distinguish between these mechanistic scenarios, we performed computational analysis on complexes of LCuOCArFCCPh (L = IPr*Me, *S*-BINAP) using dispersion-corrected DFT[57] with an ωB97X-D3 functional and the def2-TZVP basis set.[58] Geometry optimizations were conducted in a continuum solvent (benzene).[59] Details of the methodology are provided on page S42 of the ESI.†

The computed GS structure of (*S*-BINAP)CuOC(Ar^F)$_2$C≡CPh is a trigonal planar complex rather than a Cu-alkyne π complex

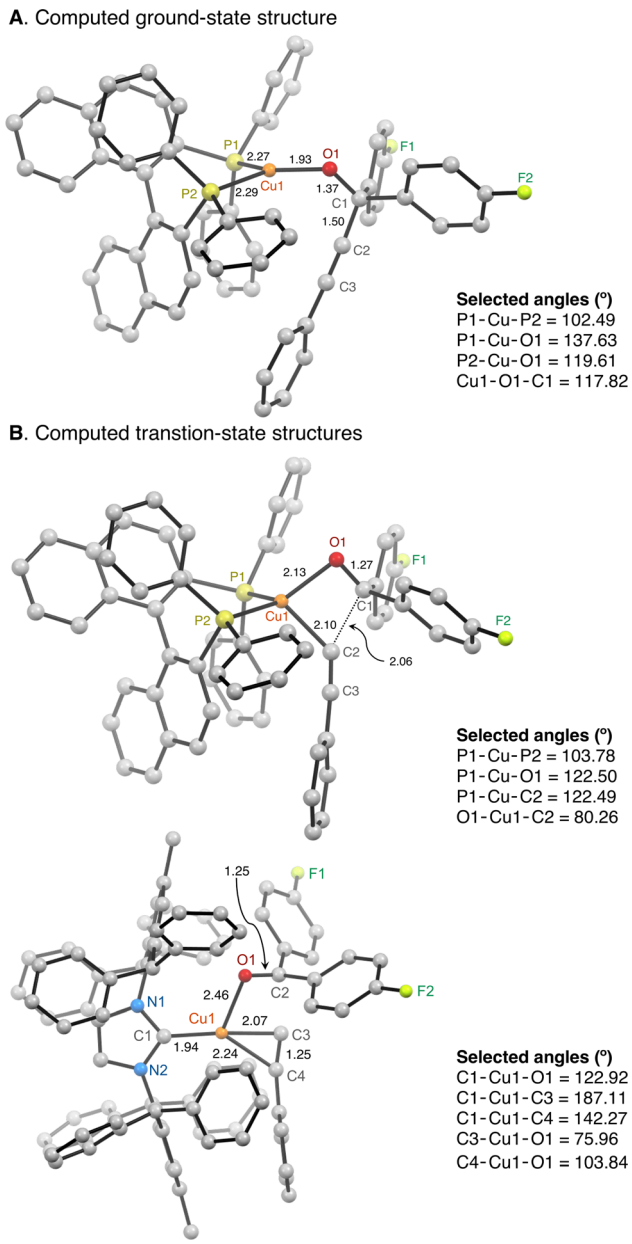

Fig. 7 Computational analysis was performed to determine the ground-state structure of (*S*-BINAP)CuOC(Ar^F)$_2$C≡CPh (A) and transition-state structures of LCuOC(Ar^F)$_2$C≡CPh complexes (L = *S*-BINAP, IPr*Me) (B) and their free energy barriers for β-alkynyl elimination. The free energy barrier for β-alkynyl elimination of a trigonal planar (*S*-BINAP)CuOC(Ar^F)$_2$C≡CPh is lowered than that of a linear (IPr*Me)CuOC(Ar^F)$_2$C≡CPh.

(Fig. 7). (*S*-BINAP)CuOC(Ar^F)$_2$C≡CPh undergoes β-alkynyl elimination with a calculated free energy barrier ($\Delta G^{\ddagger}$) of 23.5 kcal mol^{-1} compared to that of (IPr*Me)CuOC(Ar^F)$_2$C≡CPh at 24.8 kcal mol^{-1}. This small energy difference of 1.4 kcal mol^{-1} is less than the approximate energy difference of 4–5 kcal mol^{-1} based on the observed rate of β-alkynyl elimination as a function of temperature. Due to the limitations in the accuracy of the method, we also analyzed analogous complexes to establish a trend for $\Delta G^{\ddagger}$ to eliminate systematic errors in the activation free energy.

We therefore calculated the β-alkynyl elimination barrier for (IPr)CuOC(Ar^F)$_2$C≡CPh because this complex exhibits a similar β-alkynyl elimination rate to that of (IPr*Me)CuOC(Ar^F)$_2$-C≡CPh (Fig. 6) and is ligated by an IPr ligand devoid of flexible flanking aryls. A $\Delta G^{\ddagger}$ of 26.3 kcal mol^{-1} was observed for the β-alkynyl elimination of (IPr)CuOC(Ar^F)$_2$C≡CPh. A 2.8 kcal mol^{-1} increase in the $\Delta G^{\ddagger}$ for the C–C bond cleavage of (IPr)CuOC(Ar^F)$_2$C≡CPh compared to that of (*S*-BINAP)CuOC(Ar^F)$_2$-C≡CPh approaches the approximate energy difference that is consistent with experimental β-alkynyl elimination rates.

The transition-state (TS) structures for the β-alkynyl elimination of linear (IPr*Me)CuOC(Ar^F)$_2$C≡CPh and trigonal planar (*S*-BINAP)CuOC(Ar^F)$_2$C≡CPh complexes show complete C–C bond cleavage of the propargylic alkoxide as evidenced by a bond distance of 1.25–1.27 Å for the C=O functionality of Ar^F$_2$C=O (Fig. 7). The presence of monodentate IPr*Me and bidentate *S*-BINAP ligands also leads to different binding modes of the ruptured phenylacetylide. The TS structure of IPr*Me-supported species resembles a T-shaped geometry based on key angles of C1–Cu1–O1 = 122.92° and C1–Cu1–C3 = 187.11°. The Cu(I) center is additionally coordinated by an η^1-O=CArF_2 and contains a weak Cu–(η^2-C≡CPh) π interaction as evidenced by a C3–C4 distance of 1.25 Å. The computed trigonal planar (*S*-BINAP)CuOC(Ar^F)$_2$C≡CPh complex adopts a distorted tetrahedral complex in the transition state coordinated by η^1-O=CArF_2 and σ-C≡CPh ligands (Fig. 7).

We also computationally examined the electronic effect of the electron-rich SIPr ligand, which contains a saturated five-membered ring, by calculating the $\Delta G^{\ddagger}$ of β-alkynyl elimination for LCuOC(Ar^F)$_2$C≡CPh (L = IPr, SIPr) [SIPr = (1,3-bis(2,6-diisopropylphenyl)dihydroimidazolidin-2-ylidene)]. The calculated $\Delta G^{\ddagger}$ of 26.3 and 26.2 kcal mol^{-1} for (IPr)CuOC(Ar^F)$_2$-C≡CPh and (SIPr)CuOC(Ar^F)$_2$C≡CPh, respectively, suggests no electronic contribution between IPr and SIPr on the elimination rate at this level of theory. The geometries of the TS structures of LCuOC(Ar^F)$_2$C≡CPh (L = IPr, SIPr) are presented in Fig. S32 of the ESI.†

Conclusions

We have provided direct spectroscopic and structural evidence for the general, selective, and irreversible β-alkynyl eliminations of tertiary and secondary propargylic alkoxide Cu(I) complexes supported by various NHC and diphosphine ligands. The transformation tolerates substitutions of aryl, alkyl, hydrogen, aryl alkenyl, –C≡C(C$_6$H$_4$-*p*-OMe), and –C≡C(C$_4$H$_3$S) at the β-carbon of the propargylic alkoxides and exhibits selective β-

alkynyl over β-hydrogen elimination for the different secondary propargyl alkoxide Cu(I) complexes. This selectivity is attributed to the favorable formation of a Cu-alkyne π complex over a Cu–H–C σ complex and the stable product of Cu(I)-acetylide.

Eyring analysis of the β-alkynyl elimination of (IPr*Me)CuOC(Ar^F)$_2$C≡CPh supports an associative mechanism, in which C–C bond cleavage at the propargylic alkoxide proceeds through a four-centred transition state. Employing diphosphine ligands dramatically influenced the relative rate and reaction temperature for the β-alkynyl elimination of propargylic alkoxide complexes compared to the elimination rates obtained by modulating the steric and electronic properties of the NHC ligands. Computational analysis identified a lower free energy barrier for β-alkynyl elimination at trigonal planar diphosphine-supported propargylic alkoxide Cu(I) species than those of linear NHC-supported analogues. This comprehensive study of C–C bond cleavage at isolable low-coordinate Cu(I)-alkoxides serves to broaden the scope and mechanistic understanding of rarely observed β-carbon elimination of late first-row transition metals beyond that of Pd- and Rh-alkoxides.

Data availability

The datasets supporting this article have been uploaded as part of the ESI.† The computed geometries of the ground-state and transition-state structures reported in this study have been uploaded as XYZ files. All published datasets for the X-ray crystal structures in this study have been uploaded to the Cambridge Structural Database. The assigned CCDC identification numbers and the complexes in the study are as follows: CCDC 2345818 **1-Me**, 2345810 **1-OMe**, 2345819 **1-Cl**, 2345809 **2-Me**, 2345811 **2-OMe**, 2345814 **2-Cl**, 2345817 **4**, 2345816 **5**, 2345813 **8a**, 2345812 **8b**, 2345815 **9**.†

Author contributions

Ba L. Tran: conceptualization, investigation, data analysis, writing, editing, supervision. Jeremy D. Erickson: data analysis. Jack T. Fuller III: investigation, data analysis. Bojana Ginovska: supervision, writing – review & editing. Simone Raugei: supervision, writing – review & editing. All authors approved the manuscript.

Conflicts of interest

There are no conflicts to declare.

Acknowledgements

This work was supported by the U.S. Department of Energy (DOE), Office of Science, Basic Energy Sciences, Chemical Sciences, Geosciences and Biosciences Division, Catalysis Science Program, FWP 47319 and the National Energy Research Scientific Computing Center, a DOE Office of Science User Facility supported by the Office of Science of the U.S. Department of Energy under Contract No. DE-AC02-05CH11231 using NERSC award BES-ERCAP0026608.

Notes and references

1 R. M. Bullock, J. G. Chen, L. Gagliardi, P. J. Chirik, O. K. Farha, C. H. Hendon, C. W. Jones, J. A. Keith, J. Klosin, S. D. Minteer, R. H. Morris, A. T. Radosevich, T. B. Rauchfuss, N. A. Strotman, A. Vojvodic, T. R. Ward, J. Y. Yang and Y. Surendranath, *Science*, 2020, **369**, eabc3183.
2 M. R. Friedfeld, H. Zhong, R. T. Ruck, M. Shevlin and P. J. Chirik, *Science*, 2018, **360**, 888–893.
3 C. P. Delaney, E. Lin, Q. Huang, I. F. Yu, G. Rao, L. Tao, A. Jed, S. M. Fantasia, K. A. Püntener, R. D. Britt and J. F. Hartwig, *Science*, 2023, **381**, 1079–1085.
4 P. J. Chirik, K. M. Engle, E. M. Simmons and S. R. Wisniewski, *Org. Process Res. Dev.*, 2023, **27**, 1160–1184.
5 A. Fürstner, *ACS Cent. Sci.*, 2016, **2**, 778–789.
6 M. E. O'Reilly, S. Dutta and A. S. Veige, *Chem. Rev.*, 2016, **116**, 8105–8145.
7 A. D. Marchese, B. Mirabi and M. Lautens, *Synthesis*, 2023, **55**, 2285–2303.
8 M. D. R. Lutz and B. Morandi, *Chem. Rev.*, 2021, **121**, 300–326.
9 K. Nogi and H. Yorimitsu, *Chem. Rev.*, 2021, **121**, 345–364.
10 H.-F. Chow, C.-W. Wan, K.-H. Low and Y.-Y. Yeung, *J. Org. Chem.*, 2001, **66**, 1910–1913.
11 T. Nishimura, H. Araki, Y. Maeda and S. Uemura, *Org. Lett.*, 2003, **5**, 2997–2999.
12 A. Funayama, T. Satoh and M. Miura, *J. Am. Chem. Soc.*, 2005, **127**, 15354–15355.
13 X. Dou, N. Liu, J. Yao and T. Lu, *Org. Lett.*, 2018, **20**, 272–275.
14 T. Nishimura, T. Katoh, K. Takatsu, R. Shintani and T. Hayashi, *J. Am. Chem. Soc.*, 2007, **129**, 14158–14159.
15 R. Shintani, K. Takatsu, T. Katoh, T. Nishimura and T. Hayashi, *Angew. Chem., Int. Ed.*, 2008, **47**, 1447–1449.
16 K. Yasui, N. Chatani and M. Tobisu, *Org. Lett.*, 2018, **20**, 2108–2111.
17 P. Zhao and J. F. Hartwig, *Organometallics*, 2008, **27**, 4749–4757.
18 K.-L. Choo and M. Lautens, *Org. Lett.*, 2018, **20**, 1380–1383.
19 H. Yuan, Q. Zhou and J. Wang, *Org. Chem. Front.*, 2023, **10**, 2081–2094.
20 Y. Zhi, J. Huang, N. Liu, T. Lu and X. Dou, *Org. Lett.*, 2017, **19**, 2378–2381.
21 M. D. R. Lutz, V. C. M. Gasser and B. Morandi, *Chem*, 2021, **7**, 1108–1119.
22 M. D. R. Lutz, S. Roediger, M. A. Rivero-Crespo and B. Morandi, *J. Am. Chem. Soc.*, 2023, **145**, 26657–26666.
23 P. Zhao and C. D. I. J. F. Hartwig, *J. Am. Chem. Soc.*, 2006, **128**, 3124–3125.
24 G. Smits, B. Audic, M. D. Wodrich, C. Corminboeuf and N. Cramer, *Chem. Sci.*, 2017, **8**, 7174–7179.
25 M. Sai, H. Yorimitsu and K. Oshima, *Angew. Chem., Int. Ed.*, 2011, **50**, 3294–3298.
26 T. Li, Z. Wang, M. Zhang, H.-J. Zhang and T.-B. Wen, *Chem. Commun.*, 2015, **51**, 6777–6780.
27 T. Li, Z. Wang, W.-B. Qin and T.-B. Wen, *ChemCatChem*, 2016, **8**, 2146–2154.

28 X. Yan, R. Ye, H. Sun, J. Zhong, H. Xiang and X. Zhou, *Org. Lett.*, 2019, **21**, 7455–7459.
29 H. Lang, A. Jakob and B. Milde, *Organometallics*, 2012, **31**, 7661–7693.
30 J. E. Hein and V. V. Fokin, *Chem. Soc. Rev.*, 2010, **39**, 1302–1315.
31 G. Evano, K. Jouvin, C. Theunissen, C. Guissart, A. Laouiti, C. Tresse, J. Heimburger, Y. Bouhoute, R. Veillard, M. Lecomte, A. Nitelet, S. Schweizer, N. Blanchard, C. Alayrac and A. C. Gaumont, *Chem. Commun.*, 2014, **50**, 10008–100018.
32 N. K. Devaraj and M. G. Finn, *Chem. Rev.*, 2021, **121**, 6697–6698.
33 I. Ibni Hashim, T. Scattolin, N. V. Tzouras, L. Bourda, K. Van Hecke, I. Ritacco, L. Caporaso, L. Cavallo, S. P. Nolan and C. S. J. Cazin, *Dalton Trans.*, 2021, **51**, 231–240.
34 J. Díez, M. P. Gamasa, J. Gimeno, A. Aguirre, S. García-Granda, J. Holubova and L. R. Falvello, *Organometallics*, 1999, **18**, 662–669.
35 G. Hattori, K. Sakata, H. Matsuzawa, Y. Tanabe, Y. Miyake and Y. Nishibayashi, *J. Am. Chem. Soc.*, 2010, **132**, 10592–10608.
36 L. Xue, K. C. Ng and Z. Lin, *Dalton Trans.*, 2009, 5841–5850.
37 B. L. Tran, B. D. Neisen, A. L. Speelman, T. Gunasekara, E. S. Wiedner and R. M. Bullock, *Angew. Chem., Int. Ed.*, 2020, **59**, 8645–8653.
38 B. L. Tran, J. D. Erickson, A. L. Speelman and R. M. Bullock, *Inorg. Chem.*, 2023, **62**, 342–352.
39 A. Noonikara-Poyil, S. G. Ridlen, I. Fernández and H. V. R. Dias, *Chem. Sci.*, 2022, **13**, 7190–7203.
40 The reaction of isolated **2-Me** with 5 equiv. of $Ar^F{}_2C{=}O$ in C_6D_6 at 25–80 °C for 12 h also showed no reaction and no decomposition of **2-Me**.
41 L. P. Wolters and F. M. Bickelhaupt, *ChemistryOpen*, 2013, **2**, 106–114.
42 T. A. Albright, J. K. Burdett and M.-H. Whangbo, in *Orbital Interactions in Chemistry*, 2013, pp. 503–526.
43 M. Brendel, C. Braun, F. Rominger and P. Hofmann, *Angew. Chem., Int. Ed.*, 2014, **53**, 8741–8745.
44 M. Hackett and G. M. Whitesides, *J. Am. Chem. Soc.*, 1988, **110**, 1449–1462.
45 M. A. Carvajal, J. J. Novoa and S. Alvarez, *J. Am. Chem. Soc.*, 2004, **126**, 1465–1477.
46 Complex (dppf)Cu(mesityl) was generated *in situ* from the reaction of dppf and Cu-mesityl (CuMes) in C_6D_6 at 25 °C. [dppf = bis(diphenylphosphino)ferrocene]. A three-coordinate diphosphine-supported Cu(I)-mesityl complex, $[PhB(CH_2P^tBu_2)_2]$Cu-mesityl, has been spectroscopically and structurally characterized: R. C. Handford, L. Zhong and T. D. Tilley, *Organometallics*, 2022, **41**, 2631–2637.
47 Examples of spectroscopically and structurally characterized mononuclear (dppf)CuX [X = OAc, SCF_3, $N(C(O)CF_3)(Ar)$]: (*a*) C. B. Khadka, B. K. Najafabadi, M. Hesari, M. S. Workentin and J. F. Corrigan, *Inorg. Chem.*, 2013, **52**, 6798–6805; (*b*) Y. Yang, L. Xu, S. Yu, X. Liu, Y. Zhang and D. A. Vicic, *Chem.–Eur. J.*, 2015, **22**, 858–863; (*c*) X. Liu, S. Zhang and Y. Ding, *Dalton Trans.*, 2012, **41**, 5897–5902.
48 A. L. Speelman, B. L. Tran, J. D. Erickson, M. Vasiliu, D. A. Dixon and R. M. Bullock, *Chem. Sci.*, 2021, **12**, 11495–11505.
49 G. Dos Passos Gomes, G. Xu, X. Zhu, L. M. Chamoreau, Y. Zhang, O. Bistri-Aslanoff, S. Roland, I. V. Alabugin and M. Sollogoub, *Chem.–Eur. J.*, 2021, **27**, 8127–8142.
50 The synthesis and spectroscopic characterisation of (IPr*Me)CuOC(H)(Ph)C≡CPh (**9**) are provided in the ESI (Fig. S21, pages S27–S28†).
51 K. F. Lee, W. Bai, H. H. Y. Sung, I. D. Williams, Z. Lin and G. Jia, *Chem.–Eur. J.*, 2018, **24**, 9760–9764.
52 B. J. Burger, M. E. Thompson, W. D. Cotter and J. E. Bercaw, *J. Am. Chem. Soc.*, 1990, **112**, 1566–1577.
53 H. Xu, C. T. Hu, X. Wang and T. Diao, *Organometallics*, 2017, **36**, 4099–4102.
54 L. H. Shultz and M. Brookhart, *Organometallics*, 2001, **20**, 3975–3982.
55 C. L. Beswick and T. J. Marks, *J. Am. Chem. Soc.*, 2000, **122**, 10358–10370.
56 L. Falivene, Z. Cao, A. Petta, L. Serra, A. Poater, R. Oliva, V. Scarano and L. Cavallo, *Nat. Chem.*, 2019, **11**, 872–879.
57 Y.-S. Lin, G.-D. Li, S.-P. Mao and J.-D. Chai, *J. Chem. Theory Comput.*, 2013, **9**, 263–272.
58 F. Weigend and R. Ahlrichs, *Phys. Chem. Chem. Phys.*, 2005, **7**, 3297–3305.
59 A. V. Marenich, C. J. Cramer and D. G. Truhlar, *J. Phys. Chem. B*, 2009, **113**, 6378–6396.